Desalination and Water Treatment
www.deswater.com
doi: 10.1080/19443994.2014.950338

54 (2015) 1216–1225
April

Taylor & Francis
Taylor & Francis Group

Adsorptive removal of phosphate from secondary effluents in WWTPs by ZnAl layered double hydroxides granules

Xuelin Chen[a], Xiang Cheng[a,*], Dezhi Sun[a], Weifang Ma[a], Xingzu Wang[b]

[a]*College of Environmental Science and Engineering, Beijing Forestry University, No. 35, Tsinghua East Road, Beijing 100083, China, Tel. +86 138 1159 6749; email: 812173514@qq.com (X. Chen), Tel. +86 187 0155 8368; email: xcheng@bjfu.edu.cn (X. Cheng), Tel. +86 159 1092 4262; email: sdzlab@126.com (D. Sun), Tel. +86 139 1170 9575; email: mpeggy@163.com (W. Ma)*
[b]*Chongqing Institute of Green and Intelligent Technology, Chinese Academy of Sciences, No. 85, Jinyu Avenue, New North Zone, Chongqing 401122, China, Tel. +86 186 4008 1915; email: wxz123@163.com (X. Wang)*

Received 23 December 2013; Accepted 25 July 2014

ABSTRACT

Granular ZnAl layered double hydroxides (LDHs) were prepared to study the possible application of the material in phosphate removal from secondary effluents in wastewater treatment plants. The structural and phosphate adsorption properties of LDHs granules were compared with those of powder LDHs. The results of powder X-ray diffraction and Fourier transform infrared spectra show that polyvinyl alcohol as a binding agent did not change the interlayer distance of ZnAl LDHs or interact with the hydroxyl layers or interlayer anions. Although the distribution of pore size in granular ZnAl LDHs was similar to that in powder samples, the total pore volume and Brunauer–Emmett–Teller specific surface area decreased by 68.2% and 63.1%, respectively, after granulation. The phosphate adsorption capacity of granular ZnAl LDHs was to some extent lowered compared with that of LDHs powder; nevertheless, the decrease was not proportional to the reduction in the specific surface area, suggesting that physical surface adsorption was not a major pathway of phosphate uptake by ZnAl LDHs. Phosphate adsorption onto ZnAl LDHs powder was basically a two-step process: a fast uptake in 1 h and a slower uptake afterward, which fit well to pseudo-first-order models and pseudo-second-order models, respectively. Phosphate uptake by granular LDHs, however, had better agreements with intra-particle diffusion models during the entire contact time, indicating that mass transfer became the rate-limiting step in phosphate adsorption after LDHs granulation.

Keywords: Adsorption; Phosphate; Layered double hydroxides; Granule; Secondary effluent

1. Introduction

Phosphorus (P) has been recognized as one of the limiting nutrients for the control of eutrophication of water bodies [1]. Phosphorus even at a low level of 30 μg/L would stimulate algal growth in aquatic ecosystems [2]. In China, wastewater treatment plants (WWPTs) newly built or reconstructed are currently

*Corresponding author.

Presented at the 6th International Conference on the "Challenges in Environmental Science and Engineering" (CESE-2013), 29 October–2 November 2013, Daegu, Korea

subject to the discharge limit of phosphorus of 0.5 mg/L (as total P).

During the past decades, various technologies have been developed to enhance the removal of P from wastewaters, for example, activated sludge-based processes, chemical precipitation/crystallization, reverse osmosis, ion exchange, adsorption, and constructed wetlands [3–7]. For wastewaters with low levels of phosphorus, for example, secondary effluents in WWTPs, the removal efficiency of P by adsorption was shown to be satisfactory [8]. Generally, adsorption process requires simple operation and small consumption of chemicals that reduces the production of chemical sludge, thus has been considered as a cost-effective and environment-friendly technology. Adsorptive materials for phosphate removal from water environments documented in the previous literatures include red mud, iron oxides, modified activated carbon, aluminum oxide/hydroxide, calcite, zeolite [9–14].

Layered double hydroxides (LDHs) are a wide variety of layered compounds with a generic formula of $[M^{II}_{1-x}M^{III}_{x}(OH)_2][A^{n-}]_{x/n}{\cdot}yH_2O$, where M^{II} and M^{III} denote divalent and trivalent metal cations, respectively, and A^{n-} is the intercalated anion [15]. The compounds have shown to be a promising material for the adsorption of anions, including phosphate, from aqueous solutions due to the exchangeability of interlayer anions and the high charge density of the sheets [16, 17]. In recent years, LDHs with different composition and stacking patterns were studied for the removal of phosphate from various P-containing streams, for example, phosphate solutions [18, 19], seawater [20], and excess sludge liquor [21, 22]. Since LDHs are a group of compounds with great compositional diversity, different mechanisms responsible for phosphorus adsorption on LDHs were explored, which include surface adsorption, interlayer anion exchange, and reconstruction of calcined LDH precursors by "memory effect" [23, 24]. Our previous work studied the adsorptive behavior of phosphate on ZnAl LDHs and the major influencing factors [21]. However, for the real application of LDHs in water treatment industry, powder adsorbent has to be granulated for a better separation from aqueous phase.

This paper aims to study the effectiveness of phosphate removal from secondary effluents in WWTPs by ZnAl LDHs granules. The capacities and properties of phosphate adsorption by LDHs powder and granules were compared. Influence of water quality of secondary effluents on the phosphate adsorption by LDHs was discussed.

2. Materials and methods

2.1. Preparation of ZnAl LDHs powder and granules

ZnAl LDHs were synthesized by urea hydrolysis-based coprecipitation. $ZnCl_2$ (54.52 g), $AlCl_3{\cdot}6H_2O$ (48.286 g), and urea (144.144 g) were dissolved in 1 L of deionized (DI) water to prepare a mixed solution with 0.4 mol/L of Zn^{2+}, 0.2 mol/L of Al^{3+}, and a urea/(Zn^{2+} + Al^{3+}) molar ratio of 4. The homogeneous solution was then heated up to 100 ± 1℃ for 24 h with vigorous stirring in an oil bath to promote urea hydrolysis and consequently LDHs precipitation. The resulting slurry was washed thoroughly with DI water until no chloride ion was detected. The precipitate was dried at 60℃ in an oven for 48 h and was ground to fine powder.

Granular LDHs were prepared by using polyvinyl alcohol (PVA) as a binding agent. A PVA solution of 10% was obtained by dissolving a certain amount of PVA in DI water at 80℃. LDHs powder and 10% PVA were mixed completely and granulated to cylinder-shaped granules (2 mm in diameter and 4 mm in length) using an extruder. The cylindrical granules were dried at 60℃ in oven overnight and were stored in a desiccator before use.

2.2. Characterization of ZnAl LDHs

Powder X-ray diffraction (XRD) analysis of ZnAl LDHs was conducted on a Shimadzu XRD-6000 diffractometer using Cu Kα radiation (40 kV and 30 mA) at a scanning rate of 2°/min from 5° to 80°. Fourier transform infrared spectra (FT-IR) of the samples were recorded on a FT-IR spectrometer (Spectrum one, PerkinElmer) using KBr pellets in the wavenumber range of 4,000–400 cm^{-1}. Morphology of LDHs powder and granules was investigated by scanning electron microscopy (HITACHI, S-3400N) at beam energy of 15.0 kV. Specific surface area and pore property were measured by nitrogen adsorption–desorption isotherms on an ASAP 2020M instrument (Micromeritics) after the sample was degassed overnight under vacuum (10^{-5} Torr) at 90℃. The data were analyzed by the built-in software. Zeta potential was determined at different pH values on a zeta-meter (Malvern, Zetasizer Nano).

2.3. Phosphate adsorption assays

Phosphate adsorption by ZnAl LDHs was carried out in batch assays. Phosphate solutions at desired concentrations with a pH of 7.00 ± 0.01 were prepared

using a mixture of NaH_2PO_4 and Na_2HPO_4. In the adsorption assays, 0.1 g of ZnAl samples were added to serum vials containing 100 mL of phosphate solutions. The vials were then stirred thoroughly in a thermostat shaker at constant temperatures. At certain time intervals, certain amounts of the suspension were sampled and were filtrated through 0.22-μm glass fiber filter papers (Gelman A/E, Ann Arbor, USA) for examining the residual phosphate. Adsorption kinetics was determined by monitoring the concentration of phosphate at 25˚C for 80 h (to ensure equilibrium was reached based on preliminary experiments) with initial concentrations of 2, 10, and 50 mgP/L, respectively. Adsorption isotherms at 15, 25, and 35˚C were obtained by conducting the assays with initial concentrations of phosphate from 5 to 350 mgP/L.

Influences of pH and coexisting ions on the phosphate adsorption by ZnAl LDHs were evaluated by taking the water quality of secondary effluents into consideration. pH dependence of the phosphate adsorption was investigated by mixing 0.05 g of LDHs with 200 mL of phosphate solution of 2 mgP/L with pH 6–8. Adjustment of pH was done by using 1 M HCl or 1 M NaOH solutions. For studying the influences of coexisting ions, ZnAl LDHs were fully mixed with phosphate solutions of 2 mgP/L spiked with different anions (Cl^-, SO_4^{2-}) at an adsorbent dosage of 0.05 g/100 mL.

2.4. Fixed-bed adsorption experiment

Fixed-bed column adsorption of phosphate was performed in a glass column of 1.0 cm internal diameter and 5.0 cm length. Phosphate solution of 2.0 mgP/L was used as the influent to mimic WWTPs secondary effluents. The solution was introduced from the column bottom at a flow rate of 0.082 mL/min (empty bed contact time: 26.36 min) using a peristaltic pump (LongerPump Co. Ltd, Baoding, China). Water samples were collected at scheduled time intervals for phosphate analysis.

2.5. Analysis

COD and NH_4^+-N were determined by standard method (APHA, AWWA, WEF [25]). Anions (PO_4^{3-}, Cl^-, NO_3^-, and SO_4^{2-}) were analyzed using ion chromatography (ICS-3000, Dionex), which was run with an elution solution consisting of 250 mmol of NaOH and DI water with a mixing ratio of 12:88 (V/V) at a flow rate of 1.2 mL/min. pH was measured by a PHS-3C pH meter (Leici Co. Ltd, Shanghai).

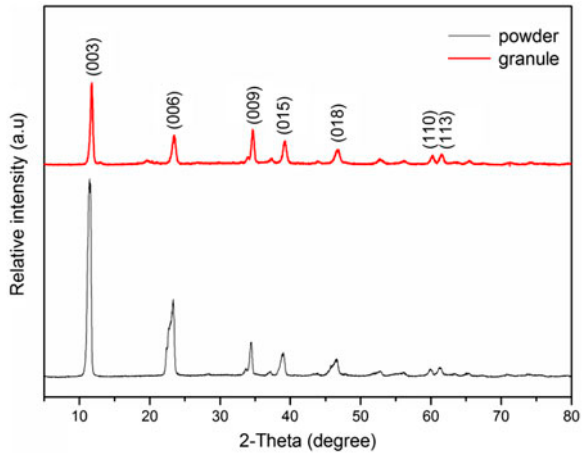

Fig. 1. XRD patterns of ZnAl LDHs powder and granules.

3. Results and discussion

3.1. Characterization of ZnAl LDHs powder and granules

XRD patterns of the prepared ZnAl LDHs powder and granule are presented in Fig. 1. Sharp peaks for (003), (006), (009), (015), and (018) planes were observed for ZnAl LDHs powder, suggesting that the sample consisted of well-defined LDHs crystallites [26]. No other solid phases were seen as impurities in the powder LDHs according to the diffraction peaks. By comparing the XRD patterns of ZnAl powder and granules, it can be concluded that the introduction of PVA in the granular ZnAl did not bring any new mineral phases into the sample. The peaks for (003) plane for the ZnAl granules was to some extent lowered, but the diffraction angle was as same as that for ZnAl

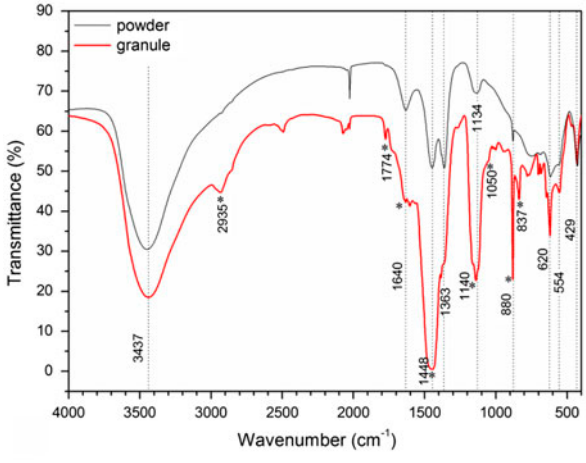

Fig. 2. FT-IR spectra of ZnAl LDHs powder and granules.

powder. This reveals that PVA molecules did not enter the interlayer space of LDHs and the hydroxyl groups in PVA did not interact with the LDHs sheets or interlayer anions either, both of which would cause a change of interlayer distance [27].

Fig. 2 shows the FTIR spectra of ZnAl LDHs samples. The broad bands centered at ~3,437 cm^{-1} can be ascribed to H-bonded stretching vibrations of the OH groups in LDHs layers. The bands at ~1,640 cm^{-1} can be assigned to the bending vibration of water molecules physically adsorbed or in the interlayer space. Three sharp peaks at 620, 554, and 429 cm^{-1} were observed in the spectra of ZnAl LDHs powder and granules, which can be interpreted as metal-oxygen vibrations [28]. Additionally, the bands of C–O vibrations were clearly seen in the IR spectrum of ZnAl powder at 1,448 (splitting of v_3), 1,363 (v_3, asymmetric stretching), 1,134 (v_3, asymmetric stretching), and 880 (v_2, out-of-plane deformation stretching) cm^{-1}, which may be due to the carbonate ions from the hydrolysis of urea during the LDHs preparation. For the granular ZnAl LDHs, characteristic bands of PVA were observed for the asymmetric stretching (2,935 cm^{-1}) and in-plane bending (1,448 cm^{-1}) vibration of C–H, out-of-plane deformation stretching (880 cm^{-1}) and asymmetric stretching (1,140 and 1,050 cm^{-1}) vibration of C–O, and stretching (1,640 cm^{-1}) and out-of-plane bending (837 cm^{-1}) vibration of C=C. The bands centered at 1,774 cm^{-1} can be due to those non-hydrolyzed vinyl acetate molecules. From the above analysis, it is apparent that the bands observed in the IR spectrum of powder LDHs were all preserved in that of granular samples and the corresponding wavelength unchanged, suggesting that the interlayer environment of ZnAl LDHs was basically not affected by the PVA-mediated granulation.

As seen in Fig. 3(a) and (b), powder ZnAl LDHs consisted of layered hexagonal crystallites with sizes in a narrow range. For the granular LDHs, many pores with different sizes were observed scattered evenly on the outer surface of the cylinder-shaped samples (Fig. 3(c)). The crystallites on the surface were broken into smaller pieces due to the extrusion operation (Fig. 3(d)). Inside the granules, however, fine

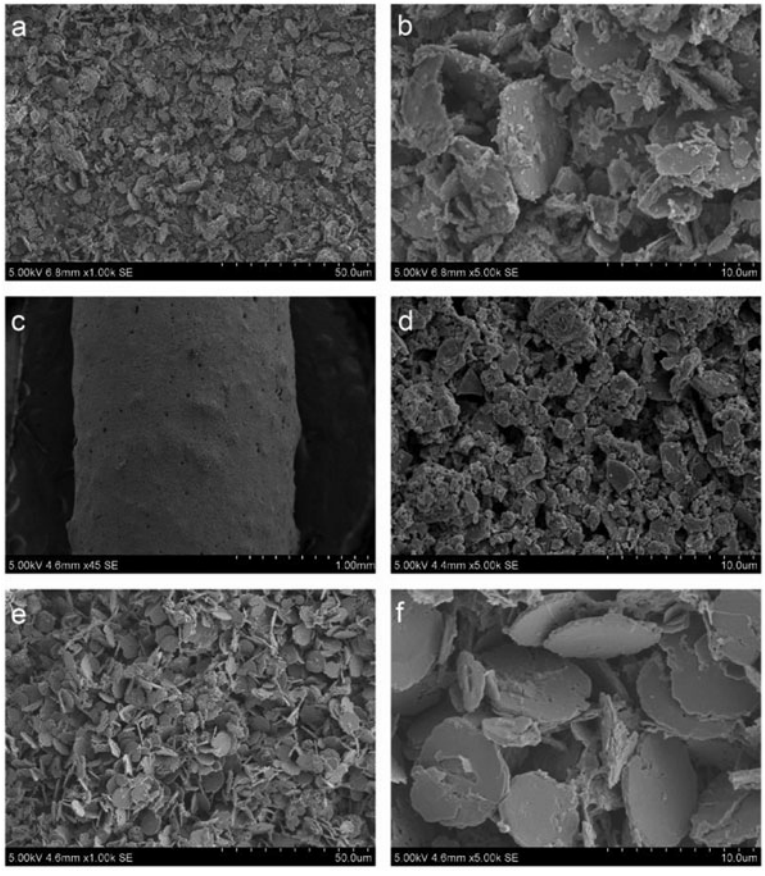

Fig. 3. SEM images of ZnAl LDHs powder ((a) and (b)) and granules (outer surface: (c) and (d); interior: (e) and (f)).

crystallites were well remained as illustrated by Fig. 3(e) and (f). A porous structure due to the arrangement of layered crystallites was clearly observed. The results demonstrate that granulation of ZnAl LDHs by PVA as a binder did not impose a noticeable influence on the LDHs micromorphology.

Nitrogen adsorption–desorption isotherms of ZnAl LDHs powder and granules are shown in Fig. 4(a). Both samples presented a type IV isotherm with a distinct H3 hysteretic loop according to IUPAC classification, which corresponds to mesoporous materials and the presence of slit-shaped pores resulted from the arrangement of layered crytallites [29]. Pore size, pore volume, and Brunauer–Emmett–Teller (BET) specific area of the samples was calculated based on Barrett–Joyner–Halenda method from the desorption branch of the isotherms and was shown in Fig. 4(b) and Table 1. The pore sizes of both powder and granular LDHs were mostly in the range of 7 to >100 nm with a small portion in the range of 2–4 nm. The total pore volumes and specific surface area decreased by 68.2% and 63.1%, respectively, after the LDHs sample was granulated.

Table 1
Specific surface area and pore properties of ZnAl LDHs

ZnAl LDHs	BET surface area (m^2/g)	Pore volume (cm^3/g)	Pore size (nm)
Powder	44.21	0.044	83.71
Granule	16.30	0.014	67.34

Fig. 5 indicates that the point of zero charge of ZnAl LDHs granules was nearly equal to that of the powder LDHs (powder: 10.5, granule: 10.8), suggesting that the use of PVA as a binder did not add extra charges to the sample surface. Under neutral pH conditions, the zeta potentials of both LDHs were positive. This can be explained by the structural positive charge on the LDHs layers and the electric double layer on the material surface. Differing from the interior structural charges on LDHs layers which are screened by interlayer anions, the surface positive charges are often not fully balanced by the adsorbed anions due to the existence of stern layer and diffusion layer [30]. The occurrence of LDHs separation from the diffusion layers would lead to a positively charged LDHs surface. In addition, at each studied pH value (except pH_{pzc}), the zeta potential of ZnAl granules was always much greater than that of powder samples. This is consistent with the fact that the addition of non-charged PVA in the material obviously decreased the charge density caused by the effect of protonation–deprotonation on the sample surface.

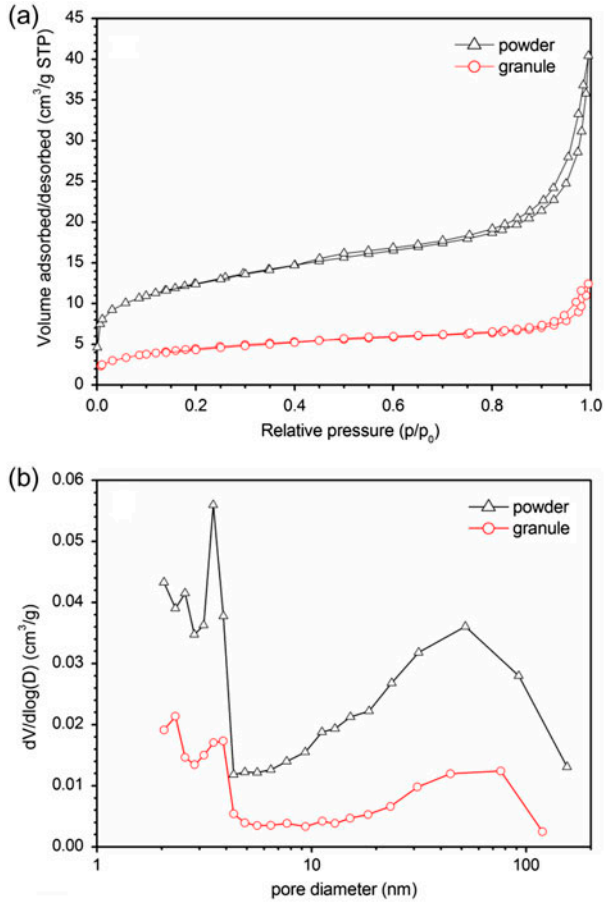

Fig. 4. N_2 adsorption–desorption isotherms (a) and pore size distribution curves (b) of ZnAl LDHs powder and granules.

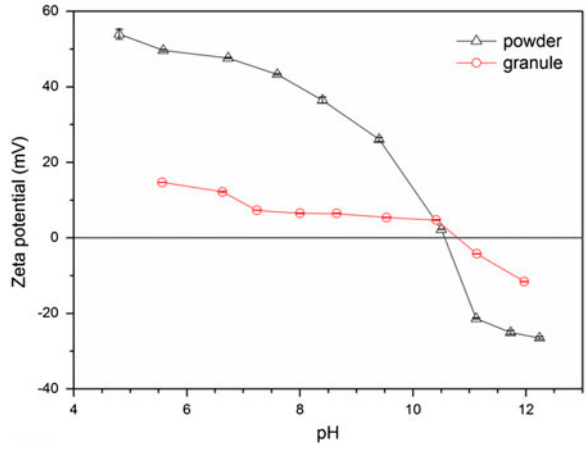

Fig. 5. Zeta potentials of ZnAl LDHs powder and granules at different pHs.

3.2. Adsorption isotherms

The adsorption capacity of granular ZnAl LDHs was to some extent lower than that of LDHs powder as illustrated by the adsorption isotherms (Fig. 6). For example, at initial concentrations of 56.9 and 192.5 mgP/L, the phosphate uptakes at equilibrium (25°C) on LDHs granules were 55.9 and 68.1% lower than those on powder samples, respectively. By comparing with the decrease in the specific surface area after granulation (being 36.9% of that of powder LDHs), it may be concluded that physical surface adsorption was not the predominant pathway of phosphate uptake by the ZnAl LDHs, especially at high phosphate concentrations. Increases in temperature adversely influenced the phosphate adsorption onto both LDHs samples. This further reveals the insignificant role of physical adsorption in the phosphate

Table 2
Langmuir and Freundlich constants for phosphate adsorption onto ZnAl LDHs powder and granules

	Langmuir equation $\frac{C_e}{q_e}=\frac{1}{bq_m}+\frac{C_e}{q_m}$			Freundlich equation $\ln q_e=\ln K_f+\frac{1}{n}\ln C_e$		
LDHs (°C)	q_m	b	R^2	K_f	n	R^2
Powder						
15	24.00	0.087	0.8842	8.14	5.07	0.9484
25	26.85	0.108	0.8118	8.82	4.73	0.9447
35	27.84	0.173	0.8072	11.45	5.81	0.9364
Granule						
15	13.36	0.021	0.9698	1.48	2.66	0.9687
25	21.09	0.034	0.8825	4.06	3.55	0.9957
35	22.68	0.070	0.8164	6.14	4.22	0.9899

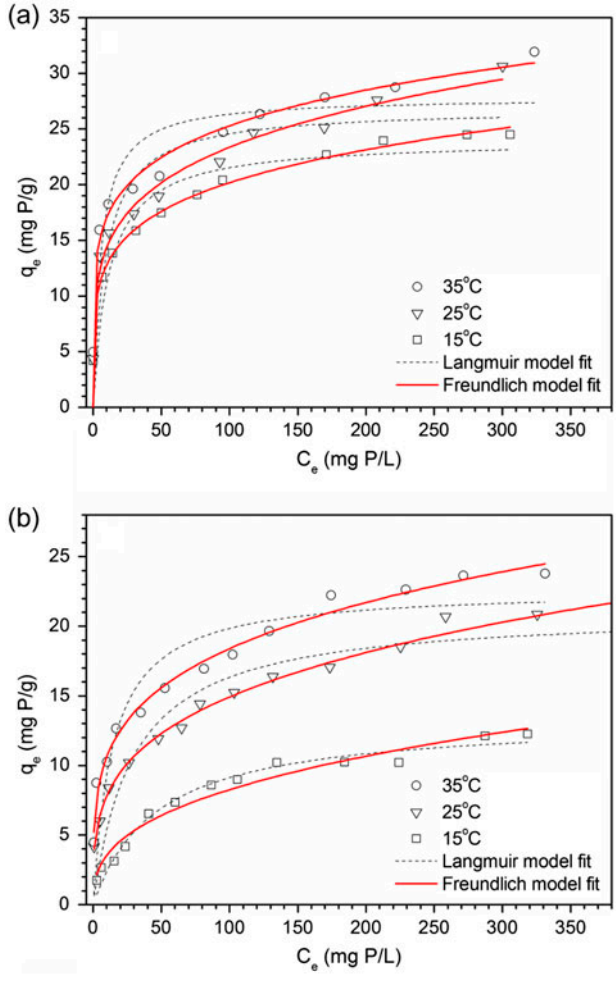

Fig. 6. Isotherms of phosphate adsorption by ZnAl LDHs and data fitting to Langmuir and Freundlich models ((a): powder; (b): granule).

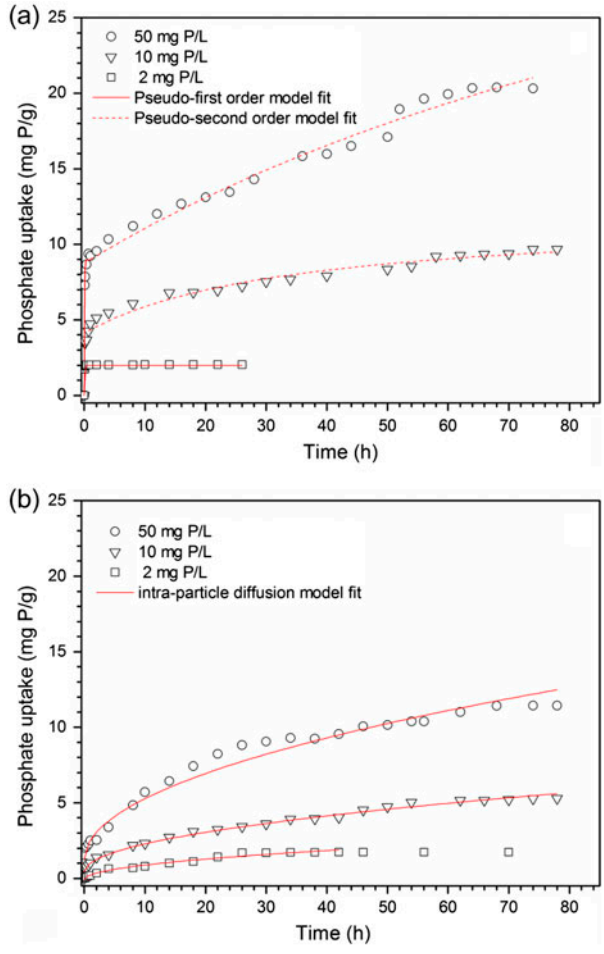

Fig. 7. Kinetics of phosphate adsorption onto ZnAl LDHs powder (a) and granules (b).

Table 3
Kinetic constants for phosphate adsorption onto ZnAl LDHs powder and granules analyzed by pseudo-first-order, pseudo-second-order and intra-particle diffusion models

	Pseudo-first-order equation			Pseudo-second-order equation			Intra-particle diffusion equation		
	$q_t = q_e - q_e e^{-k_1 t}$			$q_t = \frac{k_2 q_e^2 t}{1+k_2 q_e t}$			$q_t = k_i t^{1/2} + C$		
LDHs (mg P/L)	q_e	k_1	R^2	q_e	k_2	R^2	k_i	C	R^2
Powder (0–80 h)									
2	1.980	122.7	0.9765	2.000	147.3	0.9721	0.100	1.66	0.0854
10	8.900	0.087	0.6455	8.200	0.210	0.7708	0.760	3.24	0.8988
50	15.65	1.610	0.5186	16.33	0.120	0.6337	1.680	6.16	0.9077
Powder (0–1 h)									
10	3.870	25.02	0.9729	4.130	12.01	0.9716	4.800	0.98	0.6656
50	8.950	18.19	0.9829	9.530	3.690	0.9756	10.88	2.08	0.6979
Powder (1–80 h)									
10	5.760	0.024	0.9629	7.580	0.004	0.9726	1.480	7.53	0.9477
50	24.55	0.009	0.9720	37.85	1.7E−4	0.9798	0.580	4.50	0.9763
Granule (0–80 h)									
2	1.840	0.066	0.9812	2.300	0.029	0.9765	0.580	4.50	0.9863
10	5.180	0.049	0.9329	6.300	0.009	0.9500	0.590	0.42	0.9915
50	10.75	0.070	0.9430	12.70	0.007	0.9591	1.270	1.25	0.9745

uptake by ZnAl LDHs materials. The temperature effect on phosphate adsorption was found to be more significant by the granular LDHs, suggesting that mass transfer in the granules would be a rate-limiting step of phosphate uptake onto the material. The isotherms of phosphate adsorption by both powder and granular LDHs have better agreements with Freundlich models than with Langmuir models (see Table 2), indicating the phosphate uptake was not a monolayer surface adsorption. Multilayer or multiple-pathway adsorption of phosphate, for example, ion exchange with the interlayer Cl^-, onto the ZnAl LDHs was thus proposed as reported previously [31, 32].

3.3. Adsorption kinetics

The kinetics of phosphate adsorption on the powder and granular ZnAl LDHs apparently differed from each other as shown in Fig. 7. The phosphate uptake by ZnAl powder at initial P concentrations of 10 and 50 mg/L can be clearly divided into two steps (Fig. 7(a)): a very fast adsorption in the first hour and a relatively slow adsorption afterward. The first step of adsorption (in 1 h) can be satisfactorily described by a pseudo-first-order kinetic model (see Table 3). The rate constant (k_1) was found to be independent with the initial P concentrations, revealing that the adsorption rate was not affected by the mass transfer to the LDHs surface [27]. The second step of phosphate adsorption (after 1 h) well agreed with a pseudo-second-order model (also see Table 3). At an initial concentration of 2 mgP/L, all the phosphate was adsorbed in 20 min due to the high availability of adsorption sites at a small ratio of P/LDHs, and the adsorption data fit well in a pseudo-first-order kinetic model (also see Table 3) as at higher P concentrations. According to Fig.7(b), the two-step adsorption was not observed in phosphate uptake by granular ZnAl LDHs with all the three initial concentrations of phosphate. The adsorption during the whole contact time had better agreements with intra-particle diffusion models than other kinetic models (also see Table 3), indicating that the transfer of phosphate into the granule interior was the rate-limiting step. The intra-particle diffusion rate constant (k_i) increased with the initial P concentration increasing, which indicates the growth of driving force in enhancing the phosphate diffusion in the granule [33]. The small values of constant C reveal that a fast adsorption occurred on the outer surface in the initial period.

3.4. Effect of pH and coexisting anions on phosphate adsorption

Fig. 8 illustrated that phosphate adsorption by granular ZnAl LDHs was to some extent favorable in acidic environments. This can be explained by the enhanced affinity between phosphate ions and protonated LDHs surface as demonstrated by the pH buffer effect of LDHs and also the foregoing results of zeta potential tests (pH_{pzc}: 10.8). As can be seen in Fig. 8, phosphate adsorption by LDHs granules was still satisfactory in waters with near-neutral pH levels, for example, WWTPs secondary effluents.

Urban sewage usually contains a considerable amount of Cl^- and SO_4^{2-}, and the anions would still remain in the effluents from secondary water treatment. According to Fig. 9, the effects of these two anions at levels that commonly seen in secondary effluents on phosphate adsorption by ZnAl granules were comparable, and both of which were acceptable.

3.5. Fixed-bed column adsorption

A continuous experiment of fixed-bed column adsorption was conducted with a phosphate solution of 2 mgP/L, which was to mimic WWTP secondary effluents. From the breakthrough curve, the bed volumes of treated P-bearing solution at the breakthrough point (2 mgP/L) were 4,315 for the granular ZnAl LDHs with an accumulated adsorption capacity of 7.65 mgP/g (Fig. 10). According to the *Chinese Discharge Limits of Pollutants for Municipal Wastewater Treatment Plants (GB 18918–2002)*, newly built or reconstructed WWTPs in China since 1 July 2002 are subject to a stricter discharge limit (Grade 1A) of phosphate as low as 0.5 mg/L. Taking this discharge level into consideration, 2,200 bed volumes of phosphate solution was treated at the breakthrough point (0.5 mg/L) with an accumulated adsorption capacity of 5.04 mgP/g.

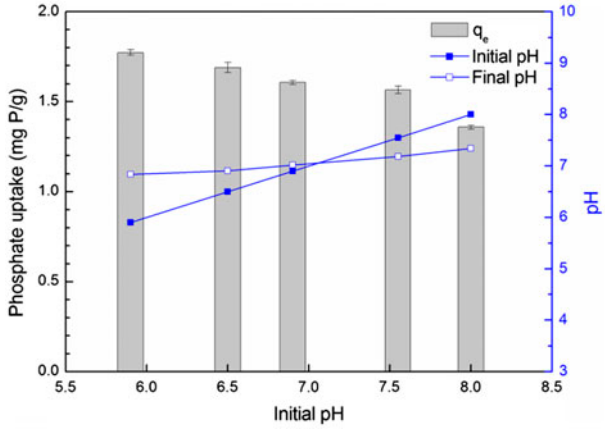

Fig. 8. Phosphate adsorption by ZnAl LDHs granules at different pH levels.

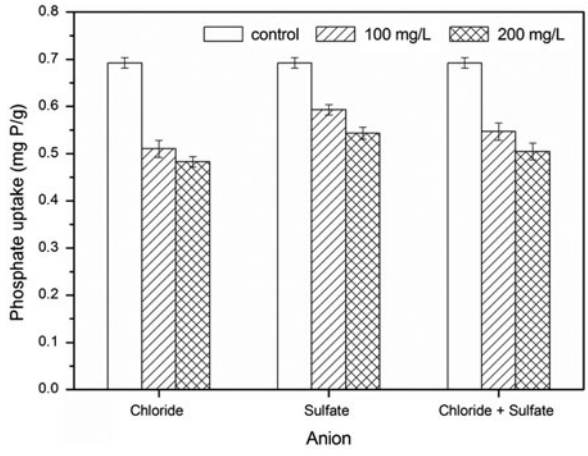

Fig. 9. Adsorption of phosphate by ZnAl LDHs granules in the presence of coexisting ions.

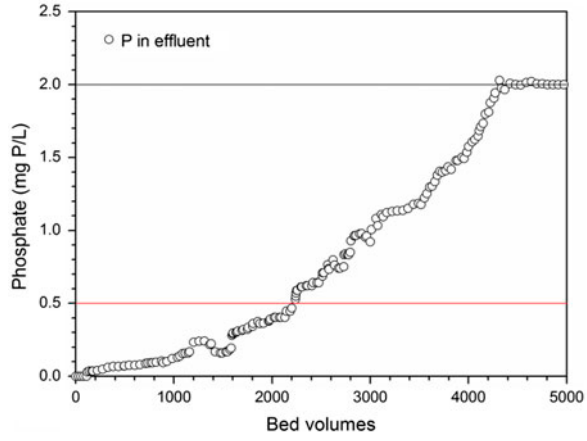

Fig. 10. Breakthrough curves of phosphate adsorption on ZnAl LDHs granules (phosphate concentration: 2 mgP/L; EBCT: 26.36 min).

4. Conclusion

This paper investigated the structure and adsorption capacity of granular ZnAl LDHs as an adsorbent for removing phosphate from WWTPs secondary effluents. The results revealed that PVA as a binder did not change the interlayer space of ZnAl LDHs or interact with the layered structure. The distribution of pore size in granular LDHs was similar to that in the powder, whereas the total pore volume and specific

surface area (BET) were reduced by 68.2% and 63.1%, respectively, after granulation. The reduction in the adsorption capacity of phosphate by ZnAl LDHs was not proportional to the decrease in the specific surface area, indicating physical surface adsorption was not a major pathway of the phosphate removal. Increases in temperature led to improvements of phosphate uptake by both ZnAl powder and granules, which also suggests the insignificant role of physical adsorption in the total removal of phosphate. Phosphate adsorption by ZnAl LDHs granules was more sensitive to temperature increases compared with the powder samples, implying that mass transfer of phosphate in the granule became the rate-limiting step of phosphate uptake. Phosphate adsorption by the powder ZnAl LDHs consisted of a fast step in the first hour and a slow step afterward, which followed pseudo-first-order models and pseudo-second-order models, respectively. However, phosphate adsorption by ZnAl LDHs granules basically agreed more with intra-particle diffusion models during the entire test. The influence of pH and coexisting anions (Cl^- and SO_4^{2-}) that commonly seen in secondary effluents was demonstrated to be small in the tested range. By fixed-bed column experiments, 2,200 bed volumes of phosphate solution of 2 mg/L can be treated at the breakthrough point of 0.5 mg/L, which is the phosphate discharge limit for newly built/reconstructed WWPTs in China.

Acknowledgements

This work was supported by the Fundamental Research Funds for the Central Universities (TD-JC-2013-3) and the National Natural Science Foundation of China (No. 51008023, No. 51008025).

References

[1] D.W. Schindler, R.E. Hecky, D.L. Findlay, M.P. Stainton, B.R. Parker, M.J. Paterson, K.G. Beaty, M. Lyng, S.E.M. Kasian, Eutrophication of lakes cannot be controlled by reducing nitrogen input: Results of a 37-year whole-ecosystem experiment, Proc. Nat. Acad. Sci. 105 (2008) 11254–11258.

[2] M.A. Zurawsky, W.D. Robertson, C.J. Ptacek, S.L. Schiff, Geochemical stability of phosphorus solids below septic system infiltration beds, J. Contam. Hydrol. 73 (2004) 129–143.

[3] A. Oehmen, P.C. Lemos, G. Carvalho, Z.G. Yuan, J. Keller, L.L. Blackall, M.A.M. Reis, Advances in enhanced biological phosphorus removal: From micro to macro scale, Water Res. 41 (2007) 2271–2300.

[4] S.K. Ramasahayam, L. Guzman, G. Gunawan, T. Viswanathan, A comprehensive review of phosphorus removal technologies and processes, J. Macromol. Sci. Part A 51 (2014) 538–545.

[5] N. Karapinar, E. Hoffmann, H.H. Hahn, P-recovery by secondary nucleation and growth of calcium phosphates on magnetite mineral, Water Res. 40 (2006) 1210–1216.

[6] J.L. Acero, F.J. Benitez, A.I. Leal, F. Real, Membrane filtration technologies applied to municipal secondary effluents for potential reuse, J. Hazard. Mater. 177 (2010) 390–398.

[7] I. Vera, F. Araya, E. Andrés, K. Sáez, G. Vidal, Enhanced phosphorus removal from sewage in mesocosm-scale constructed wetland using zeolite as medium and artificial aeration, Environ. Technol. 35 (2014) 1639–1649.

[8] X.C. Wei, R.C. Viadero, S. Bhojappa, Phosphorus removal by acid mine drainage sludge from secondary effluents of municipal wastewater treatment plants, Water Res. 42 (2008) 3275–3284.

[9] Q. Yue, Y. Zhao, Q. Li, W. Li, B. Gao, S. Han, Y. Qi, H. Yu, Research on the characteristics of red mud granular adsorbents (RMGA) for phosphate removal, J. Hazard. Mater. 176 (2010) 741–748.

[10] S.Y. Yoon, C.G. Lee, J.A. Park, J.H. Kim, S.B. Kim, S.H. Lee, J.W. Choi, Kinetic, equilibrium and thermodynamic studies for phosphate adsorption to magnetic iron oxide nanoparticles, Chem. Eng. J. 236 (2014) 341–347.

[11] Z.F. Wang, E. Nie, J.H. Li, M. Yang, Y.J. Zhao, X.Z. Luo, Z. Zheng, Equilibrium and kinetics of adsorption of phosphate onto iron-doped activated carbon, Environ. Sci. Pollut. Res. 19 (2012) 2908–2917.

[12] A.F. Sousa, T.P. Braga, E.C.C. Gomes, A. Valentini, E. Longhinotti, Adsorption of phosphate using mesoporous spheres containing iron and aluminum oxide, Chem. Eng. J. 210 (2012) 143–149.

[13] Y. Liu, X. Sheng, Y. Dong, Y. Ma, Removal of high-concentration phosphate by calcite: Effect of sulfate and pH, Desalination 289 (2012) 66–71.

[14] A. Alshameri, C. Yan, X. Lei, Enhancement of phosphate removal from water by TiO_2/Yemeni natural zeolite: Preparation, characterization and thermodynamic, Microporous Mesoporous Mater. 196 (2014) 145–157.

[15] T. Kwon, G.A. Tsigdinos, T.J. Pinnavaia, Pillaring of layered double hydroxides (LDH's) by polyoxometalate anions, J. Am. Chem. Soc. 110 (1988) 3653–3654.

[16] K.H. Goh, T.T. Lim, Z. Dong, Application of layered double hydroxides for removal of oxyanions: A review, Water res. 42 (2008) 1343–1368.

[17] K. Kuzawa, Y.J. Jung, Y. Kiso, T. Yamada, M. Nagai, T.G. Lee, Phosphate removal and recovery with a synthetic hydrotalcite as an adsorbent, Chemosphere 62 (2006) 45–52.

[18] R. Chitrakar, S. Tezuka, J. Hosokawa, Y. Makita, A. Sonoda, K. Ooi, T. Hirotsu, Uptake properties of phosphate on a novel Zr-modified MgFe-LDH(CO3), J. Colloid Interface Sci. 349 (2010) 314–320.

[19] J.B. Zhou, S.L. Yang, J.G. Yu, Z. Shu, Novel hollow microspheres of hierarchical zinc–aluminum layered double hydroxides and their enhanced adsorption capacity for phosphate in water, J. Hazard. Mater. 192 (2011) 1114–1121.

[20] R. Chitrakar, S. Tezuka, A. Sonoda, K. Sakane, K. Ooi, T. Hirotsu, Adsorption of phosphate from seawater on calcined MgMn-layered double hydroxides, J. Colloid Interface Sci. 290 (2005) 45–51.

[21] X. Cheng, X.R. Huang, X.Z. Wang, B.Q. Zhao, A.Y. Chen, D.Z. Sun, Phosphate adsorption from sewage sludge filtrate using zinc-aluminum layered double hydroxides, J. Hazard. Mater. 169 (2009) 958–964.
[22] X. Cheng, X.R. Huang, X.Z. Wang, D.Z. Sun, Influence of calcination on the adsorptive removal of phosphate by Zn–Al layered double hydroxides from excess sludge liquor, J. Hazard. Mater. 177 (2010) 516–523.
[23] K.H. Goh, T.T. Lim, A. Banas, Z.L. Dong, Sorption characteristics and mechanisms of oxyanions and oxyhalides having different molecular properties on Mg/Al layered double hydroxide nanoparticles, J. Hazard. Mater. 179 (2010) 818–827.
[24] X. Cheng, Y. Wang, Z. Sun, D. Sun, A. Wang, Pathways of phosphate uptake from aqueous solution by ZnAl layered double hydroxides, Water Sci. Technol. (2013) 1757–1763.
[25] APHA, AWWA, WEF, Standard Methods for the Examination of Water and Wastewater, twentieth ed., Washington, DC, 1998.
[26] W. Yang, Y. Kim, P.K.T. Liu, M. Sahimi, T.T. Tsotsis, A study by *in situ* techniques of the thermal evolution of the structure of a Mg–Al–CO_3 layered double hydroxide, Chem. Eng. Sci. 57 (2002) 2945–2953.
[27] B. Cheknane, O. Bouras, M. Baudu, J.P. Basly, A. Cherguielaine, Granular inorgano-organo pillared clays (GIOCs): Preparation by wet granulation characterization and application to the removal of a Basic dye (BY28) from aqueous solutions, Chem. Eng. Sci. 158 (2010) 528–534.
[28] J.G. Wang, Y. Wei, J. Yu, Influences of polyhydric alcohol co-solvents on the hydration and thermal stability of MgAl-LDH obtained via hydrothermal synthesis, Appl. Clay Sci. 72 (2013) 37–43.
[29] F. Rouquerol, J. Rouquerol, K. Sing, Adsorption by Powders and Porous Solids, first ed., Academic Press, London, 1998.
[30] Z.P. Xu, Y. Jin, S. Liu, Z.P. Hao, G.Q. Lu, Surface charging of layered double hydroxides during dynamic interactions of anions at the interfaces, J. Colloid Interface Sci. 326 (2008) 522–529.
[31] C. Forano, Environmental remediation involving layered double hydroxides, Interface Sci. Technol. 1 (2004) 425–458.
[32] S.V. Prasanna, P.V. Kamath, Synthesis and characterization of arsenate-intercalated layered double hydroxides (LDHs): Prospects for arsenic mineralization, J. Colloid Interface Sci. 331 (2009) 439–445.
[33] N.Y. Mezenner, A. Bensmaili, Kinetics and thermodynamic study of phosphate adsorption on iron hydroxide-eggshell waste, Chem. Eng. Sci. 147 (2009) 87–96.